Research Article

Dynamics of axially functionally graded pipes conveying fluid using a higher order shear deformation theory

Reza Aghazadeh [a],*

[a]*Department of Aeronautical Engineering, University of Turkish Aeronautical Association, Ankara 06790, Turkey*

ABSTRACT

This study presents a novel approach for addressing dynamical characteristics of fluid conveying axially functionally graded pipes. The variation of material properties of the pipe along axial direction is taken into account according to a power-law function. Owing to a unified expression for displacement field, the developed model can be recast into classical Euler – Bernoulli and Timoshenko tube models as well as a newly developed higher order shear deformable tube model; the latter satisfies zero-shear conditions on free surfaces, and hence yields more realistic results. The system of partial differential equations governing dynamics of fluid conveying axially functionally graded pipes is derived through utilization of Hamilton's principle. Differential quadrature scheme is used to discretize the system of differential equations and generate numerical results. Detailed numerical investigations of the current fluid-solid interaction problem elucidate the effects of material gradation pattern, transverse shear deformation distribution profile along radial direction and fluid velocity on the natural frequencies of fluid conveying functionally graded pipes. The critical fluid velocity, which is a significant design parameter, can also be determined by means of developed procedures in this study.

1. Introduction

Fluid conveying tubes/pipes are fundamental mechanical components which are extensively used in various engineering fields such as oil industries, heat exchangers, micro- and nano-technologies and so on. Due to their widespread applications, mechanical analyses of these elements have attracted researchers' considerable attention. The stability analyses and dynamics of fluid conveying pipes (FCPs) are generally investigated within the scope of a fluid structure interaction (FSI) problem. Most of the recently developed models for predicting dynamical behavior of FCPs have their basis on a study by Paidoussis [1]. According to Paidoussis [1] FCPs may exhibit two forms of instabilities as the fluid flow velocity increases, namely, flutter and divergence. A conservative system which is supported at both ends undergoes a static instability via divergence and a non-conservative cantilever pipe loses its stability in the form large amplitude vibrations known as flutter. These two phenomena have been investigated in numerous studies and have raised a great deal of interest in recent years.

In a number of studies linear [2, 3] and nonlinear [4, 5] free vibrations of FCPs have been studied. The aim of free vibration analyses is to compute natural frequencies for various flow velocities and boundary conditions and hence to examine stability of FCPs. ElNajjar and Daneshmand [6] investigated the possibility of improving the stability of vertical and horizontal FCPs by attaching one or more additional springs and/or masses at various points along the pipe. In a study by Dagli and Ergut [7], Rayleigh theory is used to examine the influence of nonclassical boundary conditions on dynamic behavior of FCPs. Abdollahi, Dehghani Firouz-abadi [8] focused on stability and flexural vibration analyses of rotating pipes undergoing simultaneous external and internal fluid loadings. In some studies, using damping devices such as eddy-current dampers, the effort have been made to stabilize FCPs when the flow velocity inside them reaches the critical value [9].

In recent years, by advances in material science and manufacturing technologies, functionally graded materials (FGMs) have found wide variety of applications from aerospace [10] to biomedical industries [11]. FGMs belong to a novel class of composite materials which are manufactured by combining the best features of two or more constituents. The volume fractions of constitutional phases vary according to a predefined profile and in the desired direction. Nowadays, these advanced composites are manufactured in various forms such as beams, plates and shells and can be reinforced by smart materials [12-15]. The superior mechanical properties of FGMs such as low stress concentration, high designability, enhanced performance in harsh and corrosive environments, and suitability for passive control purposes have made them an ideal candidate to be used in technological applications such a fluid conveying macro- and micro-pipes. Consequently, there has been a considerable focus on stability analyses of FCPs made of FGMs. Although there are large number of studies available in the literature focusing on mechanical behavior of radially, i.e. through-the-thickness, functionally graded pipes [16-23], a few effort is made to deal with axially functionally graded pipes (AFGPs) conveying fluid. However, for complicated engineering applications and especially for control purposes, AFGPs are more preferable than radial ones. Note that modeling and analysis procedures of AFGPs are somewhat different from those employed for materials possessing through-the-thickness variations in properties. For example, unlike radial ones, the stiffness and inertia coefficients appearing in governing system of equations for AFGPs are functions of longitudinal coordinate which consequently need special treat while implementing the numerical technique. Further, new terms including the length-wise derivatives of these coefficients exist in the system of equations. In order to investigate the behavior of fluid conveying AFGPs, An and Su [24] utilized integral transform technique to numerically solve the system of governing equations. Zhou, Dai [25] studied the effects of longitudinal gradation of material properties on linear dynamics of cantilevered AFGPs aiming at enhancing stability of such systems. In some studies related to stability and dynamics of the AFGPs thermal loads [26] and nonlinear effects [27] are also taken into account. A study by Mirtalebi, Ebrahimi-Mamaghani [28] is devoted to dynamical stability and intelligent control of AFGPs by use of design flexibility of FGMs.

In all abovementioned studies as well as most researches available in the literature, the displacement field of pipe are expressed based on classical Euler-Bernoulli or Timoshenko beam models. It is worth mentioning Euler-Bernoulli model ignores transverse shear stress, and Timoshenko pipe model presumes it to be constant through the thickness. Therefore, both of these traditional theories use strictly simplifying assumptions. In order to properly express displacement field, refined beam models, which satisfy no-shear conditions on the free surfaces, are developed recently. For the beams having rectangular cross-sections, various refined shear deformable models can be found in the literature [29, 30], however, there are few number of studies regarding higher order annular tubes satisfying transverse shear conditions. In this respect, Zhang and Fu [31] took the shear deformation considerations into account and established a higher order pipe model (HOPM). They also carried out static, free vibration and wave propagation analyses using newly developed model and made comparisons between new results and those of conventional approaches. To the best of author's knowledge, there is no report on the analyses of fluid conveying AFGPs on the basis of HOPM in the available technical sources. The works utilizing higher order pipe theory are merely restricted to pure structural problems of pipes/tubes. Babaei and Reza Eslami [32] employed HOPM in conjunction with modified couple stress theory to put forward a nonclassical model for investigating vibrations of buckled functionally graded tubes in thermal environment. In some studies higher order shear deformable pipe model is used to derive an accurate size-dependent system of equations for pipes based on nonlocal elasticity [33, 34]. In another study by Zhong, Fu [35] statics and dynamics of functionally graded tubes under thermal loads are studied based on refined pipe model.

The aim of the current study is to derive governing equations and associated boundary conditions regarding free vibration problem of AFGPs conveying fluid. Owing to a unified expression for displacement field used in this study, the system can be reduced to any of conventional or higher order models, i.e. Euler-Bernoulli, Timoshenko, and higher order pipe model. The latter model, to the best of author's knowledge, is used in analysis of fluid conveying pipes for the first time. The higher order pipe model satisfies shear free conditions on inner and outer surfaces and hence can result in more realistic prediction of mechanical behavior of pipes. Further, the rotary inertia is not neglected in the derivations. The pipe is assumed to be functionally graded in longitudinal direction in which material properties smoothly vary from upstream to downstream according to a power-law function. The current study seems to be one of the few number of researches investigating effects of through-the-length variations of constituents of FCPs. Differential quadrature method (DQM) is used as a numerical solution method to obtain natural frequencies in different fluid velocities. The generated results clearly elucidate the influences of fluid velocity, material gradation patterns, and geometrical dimensions upon critical flow velocity and natural frequencies of fluid conveying AFGPs.

2. Formulation

Illustrated in Figure 1 is the configuration of an AFGP conveying fluid of velocity Γ with inner and outer radii denoted by r_i and r_o, respectively, and its length is designated by L. The volume fractions of pipe constituents vary smoothly from upstream, i.e. left side, to downstream, i.e. right side. The displacement field for the pipe domain at any time t can be expressed as the following unified form:

$$u_1\left(x_1, x_3, t\right) = u\left(x_1, t\right) - x_3 w_{,x_1} + f\left(x_2, x_3\right)\gamma(x_1, t) \quad (1.a)$$

$$u_2\left(x_1, x_3, t\right) = 0 \quad (1.b)$$

$$u_3\left(x_1, x_2, x_3, t\right) = w\left(x_1, t\right) \quad (1.c)$$

where u_1, u_2 and u_3 designate the displacements of desired point along x_1, x_2 and x_3 directions, respectively. u and w denote the displacement of any point located on mid-surface $x_3 = 0$, along x_1 and x_3 directions, respectively; ",", stands for partial derivative, γ is transverse shear strain of any hypothetical point on the neutral axis x_1 and can be stated in terms of bending rotation ϕ as

$$\gamma\left(x_1, t\right) = w_{,x_1}\left(x_1, t\right) + \phi\left(x_1, t\right), \quad (2)$$

Shape function f is utilized to delineate through-the-thickness distribution pattern of transverse shear strain. Conventional pipe models, namely Euler – Bernoulli pipe model (EBPM), Timoshenko pipe model (TPM), as well as the higher order pipe model (HOPM) [31] can be retrieved by choosing one of the following expressions for f:

EBPM: $\quad f\left(x_2, x_3\right) = 0 \quad (3.a)$

TPM: $\quad f\left(x_2, x_3\right) = x_3 \quad (3.b)$

HOPM: $\quad f\left(x_2, x_3\right) = x_3 + \dfrac{x_3}{\left(r_o^2 + r_i^2\right)}\left(\dfrac{r_o^2 r_i^2}{r^2} - \dfrac{r^2}{3}\right) \quad (3.c)$

Note that the shear stress is neglected in EBPM; TPM presumes transverse shear to be constant through the thickness of the pipe; and a nonlinear shear strain and stress distribution pattern is achievable by using HOPM.

In order to establish equations of motion and boundary conditions governing dynamics of the AFGP conveying fluid Hamilton's principle is used. It postulates that

$$\delta\int_{t_1}^{t_2}\left(K - U\right)dt = 0. \quad (4)$$

U and K here are total strain energy and kinetic energy, respectively. Strain energy U of a pipe occupying a domain Ω is written as:

$$U = \frac{1}{2}\int_{\Omega}\left(\sigma_{ij}\varepsilon_{ij}\right)dV, \quad (5)$$

where σ_{ij} and ε_{ij} are components of classical stress and strain tensors. ε_{ij} is expressed in the form of the following strain-displacement relation

$$\varepsilon_{ij} = \frac{1}{2}\left(u_{i,j} + u_{j,i}\right), \quad (6)$$

and σ_{ij} can be evaluated by means of the following constitutive relation

$$\sigma_{ij} = 2\mu\varepsilon_{ij} + \lambda\delta_{ij}\varepsilon_{kk} \quad (7)$$

where λ and μ are Lame's constants and can be expressed in terms of modulus of elasticity E and Poisson's ratio v as follows

$$\lambda = \frac{Ev}{\left(1+v\right)\left(1-2v\right)}, \qquad \mu = \frac{E}{2\left(1+v\right)} \quad (8)$$

The total kinetic energy comprising those of pipe motion and fluid flow can be written in the form

$$K = K_p + K_f \quad (9)$$

where K_p and K_f are kinetic energies of pipe and fluid, respectively and can be expresses as

$$K_p = \frac{1}{2}\int_{\Omega}\rho\left\{\left(\frac{\partial u_1}{\partial t}\right)^2 + \left(\frac{\partial u_2}{\partial t}\right)^2 + \left(\frac{\partial u_3}{\partial t}\right)^2\right\}dV, \quad (10.a)$$

$$K_f = \frac{1}{2}\int_{\Omega_f}\rho_f\left\{\vec{v}_f.\vec{v}_f\right\}dV_f$$

$$= \frac{1}{2}\int_{L}\rho_f A_f\left\{\vec{v}_f.\vec{v}_f\right\}dx_1 = \frac{1}{2}\int_{L}m_f\left\{\vec{v}_f.\vec{v}_f\right\}dx_1. \quad (10.b)$$

Ω_f is the fluid domain inside the pipe; ρ and ρ_f denote mass densities of the pipe and the fluid, respectively. A_f stands for the cross-sectional area of fluid flow, and $m_f = \rho_f A_f$ is the mass per unit length of the fluid. $\vec{v}_f$ is the fluid velocity which can be expressed as the sum of velocity of the pipe $\vec{v}_p$ and flow velocity Γ relative to the pipe

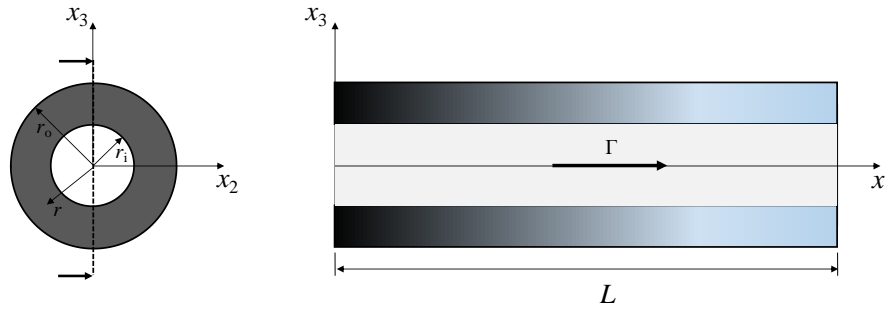$$\vec{v}_f = \vec{v}_p + \Gamma\vec{\tau} \quad (11)$$

Figure 1. Fluid conveying AFGP

$\vec{\tau}$ here is the unit vector tangent to the pipe. The components of $\vec{v}_p$ are the time derivatives of displacement field given by Eq. (1).

Note that, in the present study, a typical material property of the pipe, denoted by Z, including E, v, μ, and ρ, is assumed to be axially varying from upstream, $x_1 = 0$, to downstream, $x_1 = L$, according to the following power-law function

$$Z(x_1) = Z_0 \left[1 + \left(\frac{Z_L}{Z_0} - 1 \right) \left(\frac{x_1}{L} \right)^\alpha \right] \qquad (11)$$

α is the power-law index which characterizes the distribution profile of the material properties along axial direction of the pipe. Subscripts 0 and L designate the material properties of the pipe at $x_1 = 0$ and $x_1 = L$, respectively.

Introducing expressions for U and K and associated relations into Hamilton's principle yields the following system of governing partial differential equations:

δu :
$$A \frac{\partial}{\partial x_1} \left(\eta(x_1) \frac{\partial u}{\partial x_1} \right) = \rho(x_1) A \frac{\partial^2 u}{\partial t^2} + m_f \frac{\partial^2 u}{\partial t^2}, \qquad (12.\text{a})$$

δw :
$$(2F_{22} - I - F_{33}) \frac{\partial^2}{\partial x_1^2} \left(\eta(x_1) \frac{\partial^2 w}{\partial x_1^2} \right) + k_s (F_{55} + F_{77})$$
$$\frac{\partial}{\partial x_1} \left(\mu(x_1) \frac{\partial w}{\partial x_1} \right) - (F_{33} - F_{22}) \frac{\partial^2}{\partial x_1^2} \left(\eta(x_1) \frac{\partial \phi}{\partial x_1} \right)$$
$$+ k_s (F_{55} + F_{77}) \frac{\partial}{\partial x_1} (\mu(x_1) \phi) - m_f \Gamma^2 \frac{\partial^2 w}{\partial x_1^2}$$
$$= (2F_{22} - I - F_{33}) \frac{\partial}{\partial x_1} \left(\rho(x_1) \frac{\partial^3 w}{\partial x_1 \partial t^2} \right) + \rho(x_1) A \frac{\partial^2 w}{\partial t^2}$$
$$+ (F_{22} - F_{33}) \frac{\partial}{\partial x_1} \left(\rho(x_1) \frac{\partial^2 \phi}{\partial t^2} \right) - (c_f - 1)^2 I_f \frac{\partial^4 w}{\partial x_1^2 \partial t^2}$$
$$- c_f (c_f - 1) I_f \frac{\partial^3 \phi}{\partial x_1 \partial t^2} + m_f \frac{\partial^2 w}{\partial t^2} + 2m_f \Gamma \frac{\partial^2 w}{\partial x_1 \partial t}, \qquad (12.\text{b})$$

$\delta \phi$:
$$(F_{33} - F_{22}) \frac{\partial}{\partial x_1} \left(\eta(x_1) \frac{\partial^2 w}{\partial x_1^2} \right) - k_s (F_{55} + F_{77}) \mu(x_1) \frac{\partial w}{\partial x_1}$$
$$+ F_{33} \frac{\partial}{\partial x_1} \left(\eta(x_1) \frac{\partial \phi}{\partial x_1} \right) - k_s (F_{55} + F_{77}) \mu(x_1) \phi$$
$$= \rho(x_1)(F_{33} - F_{22}) \frac{\partial^3 w}{\partial x_1 \partial t^2} + \rho(x_1) F_{33} \frac{\partial^2 \phi}{\partial t^2}$$
$$+ c_f (c_f - 1) I_f \frac{\partial^3 w}{\partial x_1 \partial t^2} + c_f^2 I_f \frac{\partial^2 \phi}{\partial t^2}, \qquad (12.\text{c})$$

and the boundary conditions read

$$\delta u = 0 \quad \text{or} \quad A \eta(x_1) \frac{\partial u}{\partial x_1} = 0, \qquad (13.\text{a})$$

$$\delta w = 0 \quad \text{or} \quad (2F_{22} - I - F_{33}) \frac{\partial}{\partial x_1} \left(\eta(x_1) \frac{\partial^2 w}{\partial x_1^2} \right)$$
$$+ k_s (F_{55} + F_{77}) \mu(x_1) \frac{\partial w}{\partial x_1} - (F_{33} - F_{22}) \frac{\partial}{\partial x_1} \left(\eta(x_1) \frac{\partial \phi}{\partial x_1} \right)$$
$$+ k_s (F_{55} + F_{77}) \mu(x_1) \phi - m_f \Gamma^2 \frac{\partial w}{\partial x_1}$$
$$= (2F_{22} - I - F_{33}) \rho(x_1) \frac{\partial^3 w}{\partial x_1 \partial t^2} - (F_{33} - F_{22}) \rho(x_1) \frac{\partial^2 \phi}{\partial t^2}$$
$$- (c_f - 1)^2 I_f \frac{\partial^3 w}{\partial x_1 \partial t^2} - c_f (c_f - 1) I_f \frac{\partial^2 \phi}{\partial t^2} + m_f \Gamma \frac{\partial w}{\partial t}, \qquad (13.\text{b})$$

$$\delta \frac{\partial w}{\partial x_1} = 0 \quad \text{or} \quad (I + F_{33} - 2F_{22}) \eta(x_1) \frac{\partial^2 w}{\partial x_1^2}$$
$$+ (F_{33} - F_{22}) \eta(x_1) \frac{\partial \phi}{\partial x_1} = 0, \qquad (13.\text{c})$$

$$\delta \phi = 0 \quad \text{or}$$
$$(F_{33} - F_{22}) \eta(x_1) \frac{\partial^2 w}{\partial x_1^2} + F_{33} \eta(x_1) \frac{\partial \phi}{\partial x_1} = 0, \qquad (13.\text{d})$$

η, I_f, and c_f here are utilized for the sake of brevity by

letting $\eta(x_1) = \lambda(x_1) + 2\mu(x_1)$, $I_f = \rho_f \pi r_i^4 / 4$, and $c_f = f / x_3$ computed at $r = r_i$. k_s is the shear correction factor and is taken as unity for EBPM and HOPM, and for Timoshenko beam model when used for annular cross-section is given as follows [36]

$$k_s = \frac{6(\zeta^2 + 1)^2 (1+v)^2}{(7 + 12v + 4v^2)(\zeta^4 + 1) + (34 + 48v + 16v^2)\zeta^2} \quad (14)$$

where $\zeta = r_i / r_o$. The stiffness and inertia parameters appeared in Eqs. (13) and (14) are as follows

$$\{A, I, F_{22}, F_{33}, F_{55}, F_{77}, F_{15}, F_{66}, F_{99}, F_{68}, F_{88}\}$$
$$= \int_A \left\{ 1, x_3^2, x_3 f, f^2, f_{,x_3}^2, f_{,x_2}^2, f_{,x_3}, f_{,x_3 x_3}^2, f_{,x_2 x_3}^2, \right. \quad (15)$$
$$\left. f_{,x_3 x_3} f_{,x_2 x_2}, f_{,x_2 x_2}^2 \right\} dA$$

3. Numerical Solution

In the present paper, differential quadrature method (DQM) is employed to discretize and solve the system of differential equations comprising governing equations and boundary conditions [37]. The fundamental idea of DQM is to approximate m^{th} derivative of a function by a weighted sum of functional values at all sampling points. For this purpose, after dividing the domain $0 \le x \le L$ by using number of nodes N, the mth derivative of a function $z(x,t)$ with respect to x at a desired point x_i is written as:

$$\frac{\partial^m z(x,t)}{\partial x^m}\Big|_{x=x_i} = \sum_{j=1}^N c_{ij}^{(m)} z(x_j, t), \quad i = 1, 2, ..., N. \quad (16)$$

$c_{ij}^{(m)}$ are the weighting coefficients. Utilization of differential quadrature technique formulated by Eq. (16) transforms the equations of motion and boundary conditions to the following form:

$$\begin{bmatrix} \mathbf{0} & \mathbf{0} \\ \mathbf{M}_{db} & \mathbf{M}_{dd} \end{bmatrix} \begin{Bmatrix} \ddot{\mathbf{d}}_b \\ \ddot{\mathbf{d}}_d \end{Bmatrix} + \begin{bmatrix} \mathbf{0} & \mathbf{0} \\ \mathbf{C}_{db} & \mathbf{C}_{dd} \end{bmatrix} \begin{Bmatrix} \dot{\mathbf{d}}_b \\ \dot{\mathbf{d}}_d \end{Bmatrix}$$
$$+ \begin{bmatrix} \mathbf{K}_{bb} & \mathbf{K}_{bd} \\ \mathbf{K}_{db} & \mathbf{K}_{dd} \end{bmatrix} \begin{Bmatrix} \mathbf{d}_b \\ \mathbf{d}_d \end{Bmatrix} = \mathbf{0} \quad (17)$$

where $\mathbf{K}$, $\mathbf{C}$, and $\mathbf{M}$ are stiffness, damping, and mass matrices respectively. Subscripts b and d represent boundary and internal nodes, respectively. $\mathbf{d}$ is dynamic displacement vector defined by

$$\mathbf{d} = \mathbf{d}^* e^{\omega t}, \quad (18)$$

ω and $\mathbf{d}^*$ in Eq. (18) represent eigenvalue and corresponding eigenvector, respectively. Although $\mathbf{d}^*$ is a vector containing unknown amplitudes associated with u, w, and ϕ, in the current study, due to the following two reasons, axial displacement u is not taken into account in computations: 1) Inspecting governing equations and boundary conditions, it can be observed that the equations related to the axial displacement, i.e. Eqs. (12.a) and (13.a), are fully decoupled from other displacements and hence, it can be treated separately; 2) The magnitude of axial displacements are smaller than transverse ones by one order [1] and consequently they are less significant and can be neglected. Therefore, $\mathbf{d}^*$ is comprised of unknown w and ϕ values at grid points

$$\mathbf{d}^* = \left\{ \left\{ w_p^* \right\}^T, \left\{ \phi_p^* \right\}^T \right\}^T, \quad \text{for } p = 1, 2, ..., N \quad (19)$$

Substituting Eq. (18) into Eq. (17) leads to standard generalized eigenvalue problem as follows

$$\left\{ \mathbf{K} + \omega \mathbf{C} + \omega^2 \mathbf{M} \right\} \mathbf{d}^* = \mathbf{0}. \quad (20)$$

The nontrivial solution of Eq. (20) is obtained by equating determinant of coefficient matrix in Eq. (20) to zero

$$\det \left\{ \mathbf{K} + \omega \mathbf{C} + \omega^2 \mathbf{M} \right\} = \mathbf{0}. \quad (21)$$

It should be noted that eigenvalues ω which are computed through solving Eq. (21) are generally complex values in the form $\omega = \text{Re}(\omega) + i \text{Im}(\omega)$. The imaginary and real parts of eigenvalue are related to the oscillation frequency and decaying rate, respectively. $\text{Re}(\omega) > 0$ indicates that the system is unstable whereas the stability condition exists when $\text{Re}(\omega) < 0$.

4. Numerical Results

A simply supported fluid conveying AFGP is considered to carry out numerical analyses. The pipe is assumed to be functionally graded in longitudinal direction made of Epoxy at the right end with following properties: $E_L = 1.44$ GPa, $v_L = 0.38$, and $\rho_L = 1000$ kg/m³. In order to elucidate the axial material gradation effect on dynamical behavior of the pipe clearly, a material with following constants is chosen for the left hand side: $E_0 / E_L = 2$, $v_0 = v_L$ and $\rho_0 / \rho_L = 2$. In this study, for convenience, materials at the upstream and downstream ends will be called MAT1 and MAT2, respectively. The density of fluid used in numerical analysis is $\rho_f = 1000$ kg/m³ which is equal to that

of water. Unless otherwise mentioned the geometrical dimensions are taken as $r_o = 5$ cm, $r_i / r_o = 0.8$.

Plotted in

Figure **2** are the distribution profiles of material properties along dimensionless longitudinal direction x_1 / L, for different values of gradient index α. As it can be observed, a homogeneous Epoxy pipe is achieved by letting $\alpha = 0$ while as α approaches infinity a pipe made of fully MAT1 can be represented. For other values of power-law index a nonlinear pattern is seen for through-the-length variation of material properties except for $\alpha = 1$ which indicates a linear distribution profile. Further inspection of

Figure **2** reveals that at any distance x_1, the higher is the α-value, the larger is the modulus of elasticity and density.

In order to examine the accuracy of procedures and techniques employed in the current study and also conduct convergence analysis, critical flow velocities Γ_{cr}, at which instability occurs, for a homogeneous and axially functionally graded fluid conveying pipes are tabulated in Table 1. The details on how to determine Γ_{cr} are discussed in the subsequent paragraphs. The accuracy of the procedures developed can be verified by observing excellent conformity between the results produced in the present study for homogeneous pipe with those provided by Wang [38]. Although for homogeneous pipe the convergence is achieved by choosing $N = 11$, for an AFGP, 17 grid points must be employed.

Figure 3 shows first eigenvalue of fluid conveying AFGP versus flow velocity Γ, computed in different values of material power-law index α. The results are generated based on HOPM. In order to be able to comment on the results, it should be noted that when $\text{Re}(\omega) > 0$ and

$\text{Im}(\omega) = 0$ the fluid conveying pipe loses its stability due to static divergence which is generally the case in conservative pipes. The smallest flow velocity at which this condition occurs is called critical flow velocity Γ_{cr}. Thus, inspecting Figure 3, it is obvious that for the current conservative (supported at both ends) FSI problem the instability is of the divergence type. Moreover, in all material gradation patterns characterized by α, the trend is preserved. In subcritical flow region, $\Gamma < \Gamma_{cr}$, the pipe is stable. $\text{Im}(\omega)$ value computed at $\Gamma = 0$ represents natural frequency of a pipe with still water acting as a core medium where the problem is unaffected by the dynamics of fluid flow. An increase in fluid velocity results in corresponding decrease in natural frequency, i.e. imaginary part of eigenvalue, which causes the pipe configuration to approach unstable state. In order to justify this fact, it should be mentioned that the centrifugal force term $m_f \Gamma^2 \partial^2 w / \partial x_1^2$ appeared in Eq. (12.b) resembles the term resulting from axial compressive load in a beam problem. Therefore, it can be physically realized that, with increasing the flow velocity the stiffness of the pipe is diminished; in sufficiently large values of Γ the destabilizing centrifugal force overcomes the restoring flexural force and as a result divergence instability, which can also be simply called as buckling, occurs. In addition to foregoing findings, it can be seen that larger value of α which represents a pipe with higher stiffness, yields greater value of frequency and correspondingly larger Γ_{cr}. Moreover, it follows from Figure 3 that, the dynamic flutter instability occurs at velocities beyond Γ_{cr} where real and imaginary parts of ω are simultaneously positive.

Table 1. Critical flow velocities Γ_{cr} of homogeneous and AFGP conveying fluid predicted by EBPM, $L / r_o = 40$, $r_o = 100$ μm.

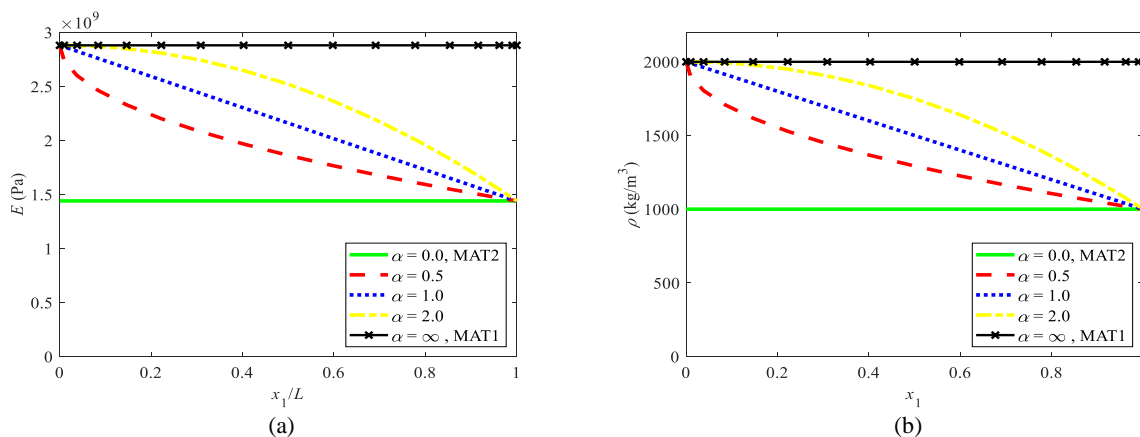| Gradient index α	Present, $N = 9$	Present, $N = 11$	Present, $N = 13$	Present, $N = 15$	Present, $N = 17$	Present, $N = 19$	Wang [38]
$\alpha = 0.0$, MAT2	45.258	45.261	45.261	45.261	45.261	45.261	45.262
$\alpha = 2.0$	76.395	76.146	76.082	76.066	76.062	76.062	-

Figure 2. Through-the-length distribution of material properties of an AFGP with $L / r_o = 40$, (a) modulus of elasticity E and (b) mass density ρ.

To study the role of geometrical parameters in the dynamics of fluid conveying AFGP, the results provided in Figure 3 are regenerated in Figure 4 by only changing length to outer radius ratio L / r_o from 40 to 60. The same conclusions mentioned in the foregoing paragraph can be drawn from Figure 4. Comparing Figure 3 with Figure 4 reveals that a longer pipe has smaller stiffness and hence possesses smaller values of natural frequencies and critical flow velocities.

Plotted in Figure 5 are the real and imaginary parts of eigenvalues computed for a thicker fluid conveying AFGP with $r_i / r_o = 0.6$. It can clearly be observed that the frequencies are increased remarkably by increasing the thickness of the pipe. This fact is expectable because the higher the thickness is the stiffer the pipe becomes.

To investigate the effects of shear deformation on the dynamical behavior of AFGP, Table 2 tabulates critical flow velocities predicted by different tube models, namely EBPM, TPM and HOPM. As it is concluded from previous results, Γ_{cr} is an increasing function of α. Since EBPM neglects transverse shear stresses, it overestimates critical flow velocities. HOPM considers a proper through-the-thickness shear stresses distribution profile and hence its results are more accurate. Although Γ_{cr} predicted by TPM are close to those computed by HOPM, a slightly smaller critical flow velocity are obtained by HOPM.
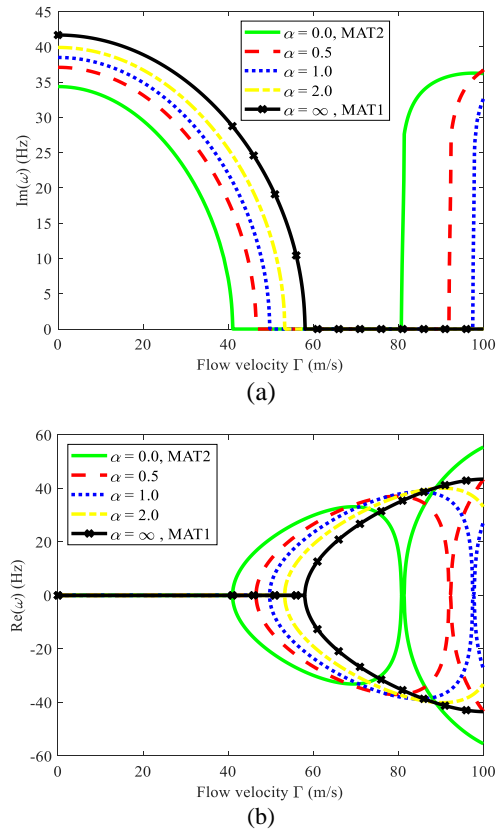

Figure 4. (a) Imaginary and (b) real parts of first eigenvalue of AFGP conveying fluid versus flow velocity Γ, $L / r_o = 60$.
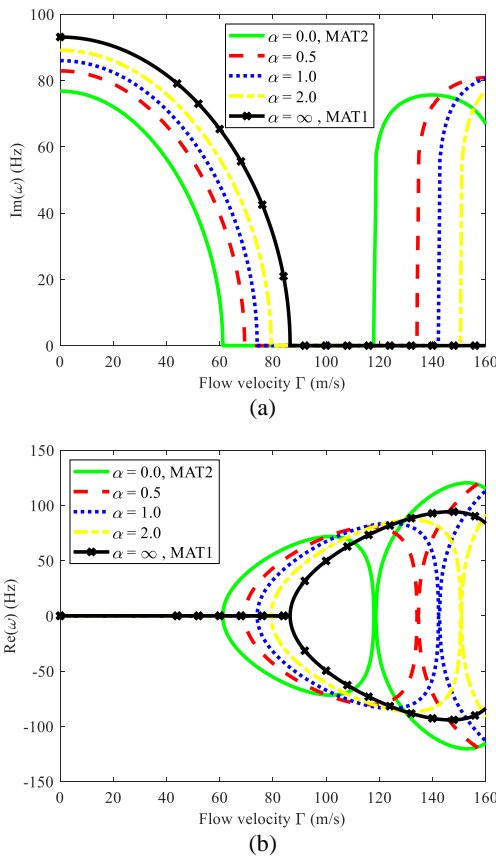

Figure 3. (a) Imaginary and (b) real parts of first eigenvalue of AFGP conveying fluid versus flow velocity Γ, $L / r_o = 40$.
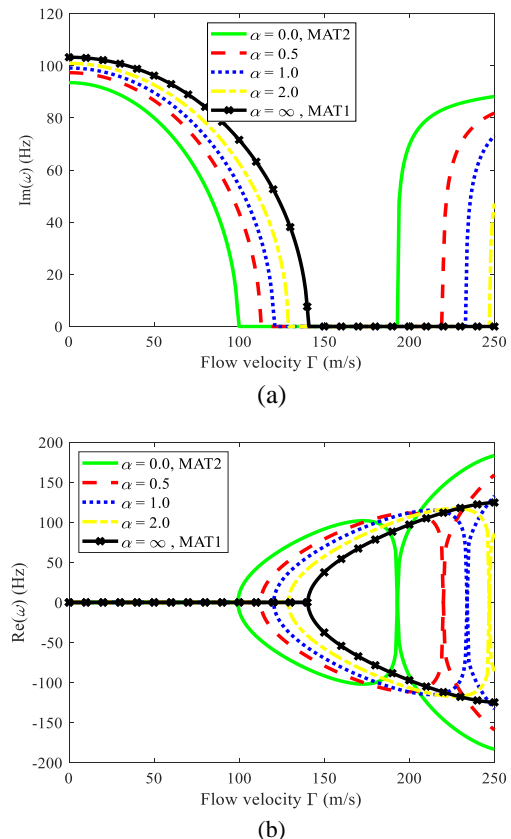

Figure 5. (a) Imaginary and (b) real parts of first eigenvalue of AFGP conveying fluid versus flow velocity Γ, $L / r_o = 40$, $r_i / r_o = 0.6$.

Table 2. Critical flow velocities Γ_{cr} of AFGP conveying fluid predicted by different tube models, $L / r_o = 40$

Model	$\alpha = 0.0$, MAT2	$\alpha = 0.5$	$\alpha = 1.0$	$\alpha = 2.0$	$\alpha = \infty$, MAT1
HOPM	61.15	69.37	74.09	79.32	86.48
EBPM	61.93	70.27	75.09	80.45	87.58
TPM	61.25	69.51	74.22	79.46	86.62

5. Conclusion

A new model for dynamical analysis of AFGPs conveying fluid is presented by employing a unified displacement field. The longitudinal variations in material properties of FCP is taken into account by employing a power law function. Using the formulation and procedures developed in the current study, it is possible to retrieve pipe models based on different theories such as Euler-Bernoulli, Timoshenko and higher order shear deformation. HOPM, which for the first time is employed in dynamics of FCPs, delineates through-the-thickness distribution profile of the transverse shear stress more realistically and therefore yields more accurate results. The DQM is utilized to conduct parametric analyses and hence to reveal the effects of geometrical and material parameters on system eigenvalues at different flow velocities.

Power law index α determines the distribution profile of the material properties through the length of pipe. The results show that it has significant effect on dynamics of fluid conveying AFGPs which can be used as an important design parameter especially in control applications. Higher values of α results in improved eigenvalues and increase critical flow velocities for divergence instability.

The differences observed between the eigenvalue results of traditional pipe models and those of HOPM postulates that employing a refined higher order tube model, which takes into account the shear deformation considerations properly, is indispensable for an accurate prediction of mechanical responses. The frequencies predicted by EBPM and TPM are larger than those generated by HOPM. EBPM yields the largest values of Re(ω) because it disregards transverse shear stresses.

It is possible to capture the influences of different material and geometrical parameters upon dynamical characteristics of AFGPs conveying fluid using the techniques developed in the current study. Owing to the superior features of functionally graded materials, the results provided in this paper can be utilized for intelligibly design and control purposes. This study also aims at providing a foundation for futures works on mechanical analyses, design, control, and optimization of FSI systems.

Declaration

The author declared no potential conflicts of interest with respect to the research, authorship, and/or publication of this article. The author also declared that this article is

original, was prepared in accordance with international publication and research ethics, and ethical committee permission or any special permission is not required.

Author Contributions

R. Aghazadeh is responsible for all section of the study.

References

1. Paidoussis, M.P., *Fluid-Structure Interactions: Slender Structures and Axial Flow*. 1998, London: Academic Press.

2. Lee, U. and J. Park, *Spectral element modelling and analysis of a pipeline conveying internal unsteady fluid.* Journal of Fluids and Structures, 2006. **22**(2): p. 273-292.

3. Xu, M.R., S.P. Xu, and H.Y. Guo, *Determination of natural frequencies of fluid-conveying pipes using homotopy perturbation method.* Computers & Mathematics with Applications, 2010. **60**(3): p. 520-527.

4. Zhang, T., et al., *Nonlinear dynamics of straight fluid-conveying pipes with general boundary conditions and additional springs and masses.* Applied Mathematical Modelling, 2016. **40**(17): p. 7880-7900.

5. Tang, Y., Y. Zhen, and B. Fang, *Nonlinear vibration analysis of a fractional dynamic model for the viscoelastic pipe conveying fluid.* Applied Mathematical Modelling, 2018. **56**: p. 123-136.

6. ElNajjar, J. and F. Daneshmand, *Stability of horizontal and vertical pipes conveying fluid under the effects of additional point masses and springs.* Ocean Engineering, 2020. **206**: p. 106943.

7. Dagli, B.Y. and A. Ergut, *Dynamics of fluid conveying pipes using Rayleigh theory under non-classical boundary conditions.* European Journal of Mechanics - B/Fluids, 2019. **77**: p. 125-134.

8. Abdollahi, R., R. Dehghani Firouz-abadi, and M. Rahmanian, *On the stability of rotating pipes conveying fluid in annular liquid medium.* Journal of Sound and Vibration, 2021. **494**: p. 115891.

9. Szmidt, T., D. Pisarski, and R. Konowrocki, *Semi-active stabilisation of a pipe conveying fluid using eddy-current dampers: state-feedback control design, experimental validation.* Meccanica, 2019. **54**(6): p. 761-777.

10. Mahamood, R.M. and E.T. Akinlabi, *Types of Functionally Graded Materials and Their Areas of Application*, in *Functionally Graded Materials*, R.M. Mahamood and E.T. Akinlabi, Editors. 2017, Springer International Publishing: Cham. p. 9-21.

11. Petit, C., L. Montanaro, and P. Palmero, *Functionally graded ceramics for biomedical application: Concept, manufacturing, and properties.* International Journal of Applied Ceramic Technology, 2018. **15**(4): p. 820-840.

12. Safaei, B., *The effect of embedding a porous core on the free vibration behavior of laminated composite plates.* Steel and Composite Structures, 2020. **35**(5): p. 659-670.

13. Moradi-Dastjerdi, R., et al., *Buckling behavior of porous*

CNT-reinforced plates integrated between active piezoelectric layers. Engineering Structures, 2020. **222**: p. 111141.

14. Fan, F., S. Sahmani, and B. Safaei, *Isogeometric nonlinear oscillations of nonlocal strain gradient PFGM micro/nano-plates via NURBS-based formulation.* Composite Structures, 2021. **255**: p. 112969.

15. Aghazadeh, R., S. Dag, and E. Cigeroglu, *Modelling of graded rectangular micro-plates with variable length scale parameters.* Structural engineering and mechanics: An international journal, 2018. **65**(5): p. 573-585.

16. Tang, Y. and T. Yang, *Post-buckling behavior and nonlinear vibration analysis of a fluid-conveying pipe composed of functionally graded material.* Composite Structures, 2018. **185**: p. 393-400.

17. Liu, H., Z. Lv, and H. Tang, *Nonlinear vibration and instability of functionally graded nanopipes with initial imperfection conveying fluid.* Applied Mathematical Modelling, 2019. **76**: p. 133-150.

18. Zhu, B., et al., *Static and dynamic characteristics of the post-buckling of fluid-conveying porous functionally graded pipes with geometric imperfections.* International Journal of Mechanical Sciences, 2021. **189**: p. 105947.

19. Dehrouyeh-Semnani, A.M., et al., *Nonlinear thermo-resonant behavior of fluid-conveying FG pipes.* International Journal of Engineering Science, 2019. **144**: p. 103141.

20. Khodabakhsh, R., A.R. Saidi, and R. Bahaadini, *An analytical solution for nonlinear vibration and post-buckling of functionally graded pipes conveying fluid considering the rotary inertia and shear deformation effects.* Applied Ocean Research, 2020. **101**: p. 102277.

21. Deng, J., et al., *Stability analysis of multi-span viscoelastic functionally graded material pipes conveying fluid using a hybrid method.* European Journal of Mechanics - A/Solids, 2017. **65**: p. 257-270.

22. Reddy, R.S., S. Panda, and G. Natarajan, *Nonlinear dynamics of functionally graded pipes conveying hot fluid.* Nonlinear Dynamics, 2020. **99**(3): p. 1989-2010.

23. Zhu, B., et al., *Nonlinear free and forced vibrations of porous functionally graded pipes conveying fluid and resting on nonlinear elastic foundation.* Composite Structures, 2020. **252**: p. 112672.

24. An, C. and J. Su, *Dynamic Behavior of Axially Functionally Graded Pipes Conveying Fluid.* Mathematical Problems in Engineering, 2017. **2017**: p. 6789634.

25. Zhou, X.-w., H.-L. Dai, and L. Wang, *Dynamics of axially functionally graded cantilevered pipes conveying fluid.* Composite Structures, 2018. **190**: p. 112-118.

26. Ebrahimi-Mamaghani, A., et al., *Thermo-mechanical stability of axially graded Rayleigh pipes.* Mechanics Based Design of Structures and Machines, 2020: p. 1-30.

27. Lu, Z.-Q., et al., *Nonlinear vibration effects on the fatigue life of fluid-conveying pipes composed of axially functionally graded materials.* Nonlinear Dynamics, 2020. **100**(2): p. 1091-1104.

28. Mirtalebi, S.H., A. Ebrahimi-Mamaghani, and M.T. Ahmadian, *Vibration Control and Manufacturing of Intelligibly Designed Axially Functionally Graded Cantilevered Macro/Micro-tubes.* IFAC-PapersOnLine, 2019. **52**(10): p. 382-387.

29. Şimşek, M. and J.N. Reddy, *Bending and vibration of functionally graded microbeams using a new higher order beam theory and the modified couple stress theory.* International Journal of Engineering Science, 2013. **64**: p. 37-53.

30. Aghazadeh, R., E. Cigeroglu, and S. Dag, *Static and free vibration analyses of small-scale functionally graded beams possessing a variable length scale parameter using different beam theories.* European Journal of Mechanics - A/Solids, 2014. **46**: p. 1-11.

31. Zhang, P. and Y. Fu, *A higher-order beam model for tubes.* European Journal of Mechanics - A/Solids, 2013. **38**: p. 12-19.

32. Babaei, H. and M. Reza Eslami, *Size-dependent vibrations of thermally pre/post-buckled FG porous micro-tubes based on modified couple stress theory.* International Journal of Mechanical Sciences, 2020. **180**: p. 105694.

33. She, G.-L., et al., *Nonlinear bending and vibration analysis of functionally graded porous tubes via a nonlocal strain gradient theory.* Composite Structures, 2018. **203**: p. 614-623.

34. She, G.-L., et al., *On buckling and postbuckling behavior of nanotubes.* International Journal of Engineering Science, 2017. **121**: p. 130-142.

35. Zhong, J., et al., *Nonlinear bending and vibration of functionally graded tubes resting on elastic foundations in thermal environment based on a refined beam model.* Applied Mathematical Modelling, 2016. **40**(17): p. 7601-7614.

36. Hutchinson, J.R., *Shear Coefficients for Timoshenko Beam Theory.* Journal of Applied Mechanics, 2000. **68**(1): p. 87-92.

37. Sahmani, S. and B. Safaei, *Large-amplitude oscillations of composite conical nanoshells with in-plane heterogeneity including surface stress effect.* Applied Mathematical Modelling, 2021. **89**: p. 1792-1813.

38. Wang, L., *Size-dependent vibration characteristics of fluid-conveying microtubes.* Journal of Fluids and Structures, 2010. **26**(4): p. 675-684.